

TXRF and ICP-OES analysis of liquid-phase laser-ablated (LP-LA) nanoparticles of cryolite-alumina solutions

Ricardo Castell · Eduardo D. Greaves ·
Lyzeth Abdala · Haydn Barros

Received: 29 April 2012 / Published online: 22 September 2012
© Springer-Verlag 2012

Abstract A new procedure with minimum sample preparation has been developed for a fast and serial analysis of cryolite with varying concentrations of dissolved alumina by liquid-phase laser ablation followed by Total Reflection X-Ray Fluorescence and induced coupled plasma optical emission spectroscopy. The analysis supplies the sodium/aluminium ratio of bath samples taken from industrial Hall-Herault reduction cells, as well as trace element relative concentrations. Two different types of molten samples taken directly from the aluminium production plant were placed under distilled de-ionized water in a quartz cell and subjected to pulsed laser ablation using the beam from a third harmonic Nd:YAG laser. Scanning electron microscopy examination shows the nanoparticles nature of the ablated material. The water-suspension is deposited on quartz reflectors for Total Reflection X-ray Fluorescence analysis or directly aspirated to the induced coupled plasma yielding the aluminium and sodium signals. Instrument quantification of the elements is performed by the use of aqueous standards. Validation tests were done with cryolite sample digestion and standard methods of sample quantification. The procedure can provide the aluminium/sodium ratio with adequate precision for aluminium production plant cell diagnostics and reveals the trace elements that could be considered as contamination.

1 Introduction

Laser ablation coupled with induced coupled plasma (LA-ICP) is a technique that has elicited much discussion

in the literature [1–4]. It is claimed [2] that “due to its versatility and inherent sensitivity LA-ICP spectrometry certainly represents one of the most attractive methods for spatially resolved analysis of solids”. As carried out in these references, intense pulses of IR light, typically of 775 nm wavelength, of short (tens of nanoseconds) or ultra-short (hundreds of femtoseconds) pulses are impinged on the specimen under scrutiny with repetition rates of the order of 10 Hz. The laser power output may vary to modify the fluence (energy per unit area deposited). The laser pulse impact on the target produces plasma that removes material from the sample. This results in the production of small or very small particles that, ideally, should be representative of the composition of the bulk sample. The particles so produced are transported by an inert carrier gas (Helium or Argon) to the ICP spectrometer plasma torch. The procedure is capable of dealing in a simple manner with the analysis of solid materials such as ceramics, glasses, some minerals, special super alloys and refractories which are very difficult to analyse due to the difficulty of rendering the material into solution.

A lot of work has gone into the size, shape and composition of the material produced by the ablation process and on the transportability of such material to the plasma torch. A large number of factors of the experimental setup are studied and optimized to improve the efficiency and accuracy of the analysis [5–12].

The production of particles which may be segregated during the gaseous phase transport due to gravity or inertial factors has to be avoided. Also, laser-induced fractionation may result from the thermal character of nanosecond LA involving processes such as preferential evaporation, which holds risk of material redistribution, and cumulative enrichment or depletion of certain constituents. These factors can affect the representativity of the transported

R. Castell · E. D. Greaves (✉) · L. Abdala · H. Barros
Universidad Simon Bolivar, Apartado 89000,
Caracas 1080, Venezuela
e-mail: egreaves20002000@yahoo.com

aerosol and compromise the analytical result. A further problem that may take place is the occurrence of so-called memory effects. With certain instrument setups particulate matter of previous analysis remains in the transport system and reports in a following assay. The lack of adequate reference materials and the phenomena of element fractionation lead to questions of reliability of analysis when dealing with a diverse class of materials.

Liquid phase laser ablation (LP-LA), consisting of the ablation of a solid sample while under a liquid, has a great number of advantages over LA in a gas phase. The liquid has the property of trapping and containing all the ablated material in the form of a liquid suspension or as dissolved ions. The production of element segregation in the plasma during the ablation process or the production of size fractionation does not represent analytical difficulties with possible simple and adequate post ablation treatment of the liquid sample. Furthermore, the difficulty of adequate standardization by matrix matching in LA-ICP might be overcome with LP-LA as normal well-established methods of solution standardization can be applied in both, ICP-OES and ICP-MS as well as TXRF or indeed some other techniques of solution assay. Nevertheless, full quantification is still not possible.

The intimate process of liquid phase laser ablation is still a subject of work, and the production of nano-sized particles is extensively reported [13–15 and references therein]. The liquid adjacent to the laser pulse impact zone has a largely enhanced containment effect on the sample removal process due to the much higher inertial mass of the liquid as compared with a gas phase ablation. In this work we use LP-LA for the analysis of cryolite (F_6AlNa_3), a difficult material for analysis. Cryolite is used for the reduction of alumina (Al_2O_3) to metallic aluminium by the well-known Hall-Herault process [16–18]. This is a high-temperature electrolytic process that uses the Hall-Herault reduction cells. The electrolyte is a bath of fused salts consisting of a mixture of the hexafluoride of aluminium and sodium as major components and additives such as aluminium fluoride, AlF_3 , used to reduce the melting point of the cryolite. The cell operates at about 950 °C using graphite anodes and molten aluminium as a cathode. Alumina is added intermittently to the electrolytic bath whereas the aluminium is produced continuously. This results in a periodic fluctuation of the aluminium ions contained in the bath. The operation of the cell depends on many factors which determine the efficiency of the reduction process. Among these factors is the aluminium ionic concentration with a strong influence on the electrical resistance of the cell, increasing it for values in excess or for values in defect of a concentration that results in a minimum in the cell resistance. It follows that for a given current intensity the dissipated power, $P = I R^2$, has a least

value for the concentration that minimizes the resistance. Due to this and other effects [16] there is a clear economic interest in the fast determination of the aluminium concentration in the electrolytic bath, particularly in Al producer countries.

The analysis of refractory materials such as cryolite is a problem due to the difficulty of rendering the specimen in solution. Various methods developed by the industry have been used in the past such as the determination of aluminium (ISO 2367:1972, gravimetric method) and sodium (ISO 2366:1974, by Atomic Absorption Spectrometry, AAS). Methods using AAS and induced coupled plasma-optical emission spectrometry (ICP-OES) require rendering the test specimen into an adequate solution demanding expensive equipment and time-consuming chemical digestion procedures due to the refractive nature of the material. In an attempt to avoid the digestion of the cryolite samples we developed with the Venezuelan industry ALCASA [19] a method that uses a delayed gamma neutron activation analysis (NAA). The method demands a very simple sample preparation procedure. However, NAA requires the use of either a neutron generator, a nuclear reactor facility or, as reported in [19], a graphite-moderated radioisotope neutron source that unfortunately decays with time. In this paper we describe a new method for analysis of refractory materials using liquid-phase laser-ablation followed by SEM, TXRF and ICP-OES. We apply the procedure to cryolite-alumina solutions and thus avoid some of the shortcomings discussed previously.

2 Experimental

2.1 Samples

Samples used in this work were collected at an aluminum production plant (ALCASA, Puerto Ordaz, Venezuela). Sample A was collected from material at a reduction cell under repair. Sample B was taken directly from the melt at an operating reduction cell by a cell sampling procedure: The molten electrolyte collected in a steel sampling cup was allowed to cool, freeze and dislodged. The cylindrical material was broken and a specimen selected for laser ablation.

Before placing in the ablation cell the specimens were thoroughly cleaned in distilled deionised water to remove any surface contamination due to the long storage of these samples.

2.2 Laser ablation

The experimental ablation setup used in this work is shown in Fig. 1. A polarized Nd:YAG laser (Quantel, Brilliant B)

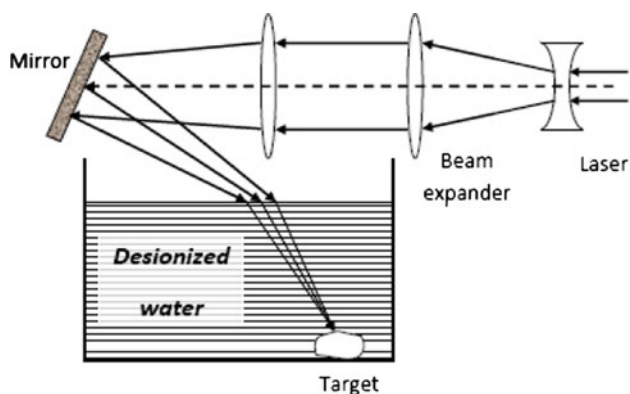


Fig. 1 Schematic diagram of pulsed laser ablation for growing cryolite nanoparticles in deionised water environment



Fig. 2 Wavelength dependence of the water absorption coefficient [22]. The range chosen for the ablation tests was near the minimum at 355 nm

operating at a wavelength of 355 nm with pulse duration of 6,7 ns (FWHM) and a repetition rate of 10 Hz was focused onto the sample through an optical system composed of a group of quartz lenses and an UV mirror. The target was immersed in distilled, deionised water and placed at the bottom of a rectangular quartz cell (width: 10 mm, length: 40 mm, height: 60 mm). The Laser wavelength was chosen to be at the best range for high transmission in water (See Fig. 2). Brewster angle incidence was considered to minimize laser light reflection at the air–water interface. Both the cryolite target and the container were rinsed with ethanol and acetone followed by pure water prior to the ablation process.

Ablation was done on the samples A and B with programmed number of shots which varied between 5 and 9,000 and laser fluencies of 480 J/cm² to ensure the

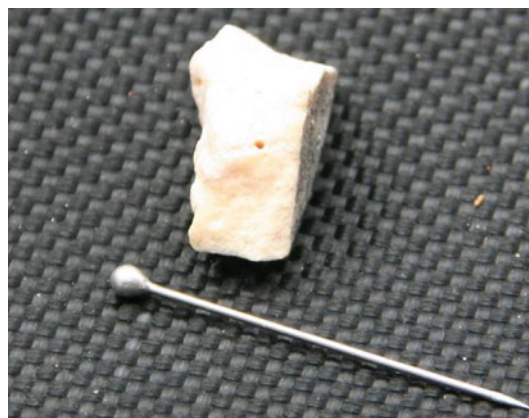


Fig. 3 Photograph of a cryolite sample showing the pit after material removal by the laser impacts

conditions needed to produce nanoparticles [15, 20]. The pulsed-laser ablation process provides fast heating of the cryolite target and is usually accompanied by boiling of the water layer adjacent to the target surface to form vapour bubbles. The depth of liquid layer on the top of the target material was kept at least 3 cm to avoid any material from the colloidal solution to be ejected by water splashing produced by the laser ablation-induced shock wave. After the ablation process, the liquid as well as two rinsing, were collected into a flask and volume determined by weighting in an analytical balance (Mettler AE 240). Samples for elemental analysis were taken to 35 ml.

Significant amounts of material were removed by the ablation procedure, see Fig. 3. Nevertheless, attempts to quantify the amount of material removed by weighting specimens before and after ablation were unsuccessful in providing the necessary accuracy.

2.3 Specimen characterization

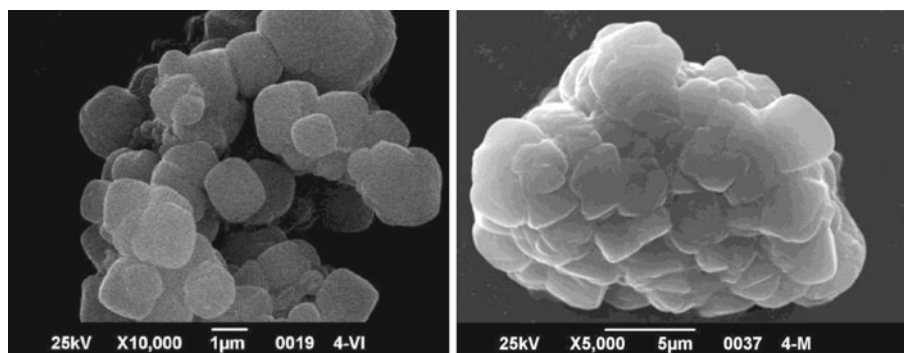
2.3.1 Optical microscopy

Samples of the liquid after laser ablation were inspected by an optical microscope to examine the ablated material. Drops of the liquid were dried on clean glass slides and seen in transmitted light in a microscope fitted with a digital camera connected to a PC computer (A KRÜSS OPTRONIC, Germany $\times 10$ to $\times 400$). No particles were observed even at the higher magnification leading to an upper size limit of a few μm for the material in the liquid after laser ablation.

2.3.2 Scanning electron microscopy (SEM)

Samples of the liquid after laser ablation were inspected by a scanning electron microscope (JSM 6390, JEOL Ltd. Japan). A 5- μL drop of the liquid in the ablation cell was

Fig. 4 SEM images of laser-ablated cryolite particles



placed in the microscope sample holder and allowed to air dry. A thin layer of carbon was sputtered and specimens observed in the microscope. Images were obtained of several fields of both cryolite samples. See Fig. 4. The images show that the LP-LA process does indeed produce sub micrometer sized particles. Individual nanosized particles as well as clusters of particles were observed in the laser-ablated material from both samples.

2.4 SEM-XRF elemental analysis

Selected particles observed in the SEM were analysed with the X-Ray Fluorescence analyzer facility of the microscope with an energy resolution of 137 eV. (Oxford Instruments INCA X-Sight. Abingdon, Oxfordshire, UK). The system is capable of detecting and measuring light elements beginning with boron. Hence good signals were obtained of the main constituents of cryolite: fluorine, sodium and aluminium.

2.5 TXRF elemental analysis

Analysis was performed with the bench top TXRF spectrometer S2 PICOFOX (Bruker AXS, Madison, WI, USA). This instrument is equipped with an air-cooled, low-power, 50 kV X-ray tube (Mo target), a multilayer monochromator with 80 % reflectivity and a liquid nitrogen-free XFlash[®] Silicon Drift Detector (SDD) with an energy resolution of <150 eV (Mn K α). Sample irradiations were done with the X-ray tube at 50 kV and a 1-mA current for 100 s. The spectrometer is able to measure elements from silicon or higher atomic weights. Hence the, all important, analysis of sodium and aluminium for these samples could not be carried out. However, all other minor and trace elements contained in the cryolite were measured.

Samples for TXRF analysis were the same solutions obtained by digestion for ICP as well as the liquid suspensions resulting from the laser ablation procedure. Sample preparation consisted in all cases in collecting an aliquot of 490 μ L after suitable agitation, in an Eppendorf vial and adding as internal standard 10 μ L of Ti 1,000 mg/L

solution. Homogenization was done with an orbital shaker. (MS3 Digital by IKA Works Inc. Wilmington, NC, USA). 10 μ L of standardized sample was deposited on clean, 30 mm diameter, quartz sample carriers (optical quality) and dried.

2.6 ICP-OES elemental analysis

ICP-OES analyses were performed for Al and Na to determine the Na/Al ratio which is important for control of the Al production process as mentioned earlier. The aliquots were taken from the 35 ml of the liquid recovered from the laser ablation cells. The different solution aliquots were aspirated directly into the ICP torch of the instrument (Spectro Ciros CCD, SPECTRO Analytical Instruments GmbH, Kleve, Germany) and quantified with the instrument's software, following standardized methods and making use of certified standards for the required calibrations. The wavelengths of the corresponding spectrometric lines that were used for the analysis were Na: 589,592 nm and for Al 396,152 nm.

3 Results and discussion

Figure 5 shows a sample XRF spectrum produced by SEM and Table 1 shows analysis results for Na and Al obtained by focusing on particles or in clusters. As expected concentration values fluctuate widely due to the small size of the particles and non representativity of the individually analysed material in addition to the coarse precision of the applied technique. However, the values obtained do not radically depart (~ 20 % SD) from the expected cryolite composition which would be obtained in the analysis of bulk material.

It is important to mention that the aforementioned results correspond to relative concentrations, since not all the elements presents in the sample are detected by this technique. That is the reason for the apparent no relation between the number of laser shots and the elemental concentrations. However, this does not affect the obtained

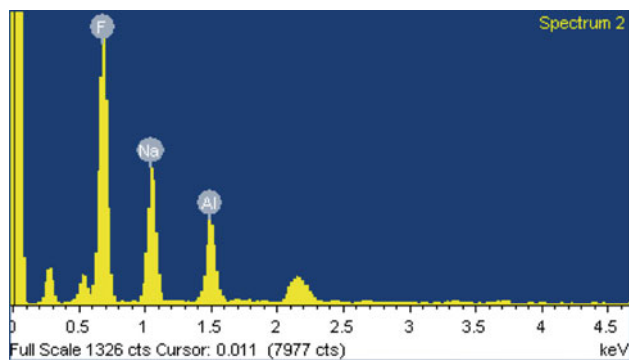


Fig. 5 Spectrum of laser-ablated particles showing the SEM-XRF signals of cryolite constituent elements

Table 1 Cryolite semi-quantitative analysis by SEM-XRF of ablated particles

Sample	Analysis results (Weight %)		
	Sodium	Aluminium	Na/Al
A (II-2) 6,000 Shots	27.1	11.4	2,4
A (II-2) 6,000 Shots	31.2	14.6	2,1
A (3-XVI) 9,000 Shots	31.7	18.4	1,7
A average			2,1
SD			17 %
B (4-M) 3,000 Shots	31.7	16.1	2,0
B (4-M) 3,000 Shots	26.3	11.6	2,3
B (4-IV) 6,000 Shots	25.9	11.2	2,3
B (4-IV) 6,000 Shots	26.5	11.6	2,3
B (4-IV) 6,000 Shots	32.6	16.6	2,0
B (4-XV) 7,200 Shots	20.6	11.2	1,8
B (4-XV) 7,200 Shots	27.1	17.2	1,6
B (6-XIII) 9,000 Shots	28.7	8.8	3,2
B (6-XIII) 9,000 Shots	33.9	11.5	2,9
B (6-XIII) 9,000 Shots	39.5	15.6	2,5
B average			2,3
SD			21 %

Na/Al concentration ratios, since it implies just a normalization factor.

Figure 6 shows a typical TXRF spectrum of the laser-ablated liquid suspension. A number of detected elements are present in the cryolite sample analysed (type A in this case). The molybdenum and its Compton peak signals come from the primary radiation of the X-ray tube used.

LA-ICP has been widely used to determine elemental or isotopic concentrations rather than absolute values of concentrations due to the difficulty in determining with good precision the amount of ablated mass from the sample studied. For quantification of concentrations use is made of matrix-matched standards [21]. However, good results can be obtained while quantifying relative concentrations.

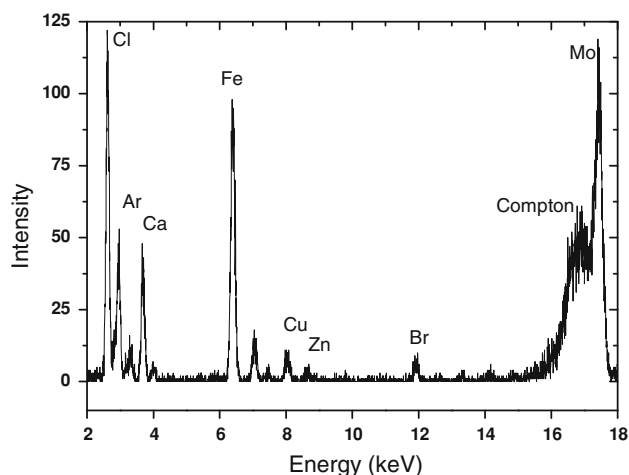


Fig. 6 TXRF spectrum of LP-LA sample of cryolite showing minor and trace elements detected

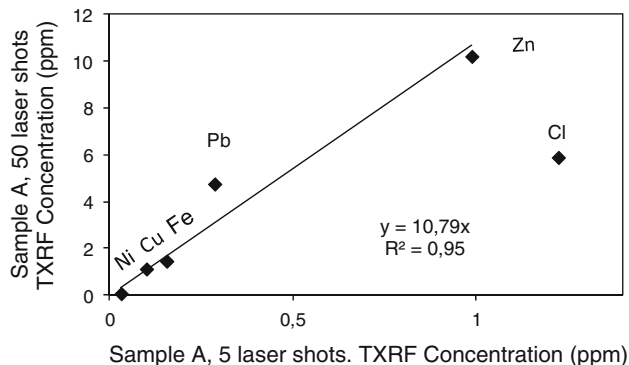


Fig. 7 TXRF analysis of Type A cryolite liquid phase laser-ablated solutions. The Cl data point was not used to produce the tendency curve. Error bars <5 % not shown

Several experiments were performed with a varying number of laser shots to optimize the procedure. As an example, in Fig. 7 it is shown that even for minor and trace elements a good correspondence between the relative concentrations of the suspensions is obtained. Particularly in this graph it is shown the TXRF elemental analysis of two liquid samples, the first one was obtained after five laser shots and the second one produced with 50 laser shots. It can be seen that the general relation for the elements is near a factor of 10, which is related with the number of the shots. The only element that does not follow that tendency is chlorine, which probably forms gaseous molecules at higher temperatures (due to the number of shots) and probably escapes from the solution. This information can be of use when evaluating possible contamination of the cryolite used in the industrial Al production process.

As mentioned earlier, the quantitative determination of the concentration ratio Na/Al is very important. These

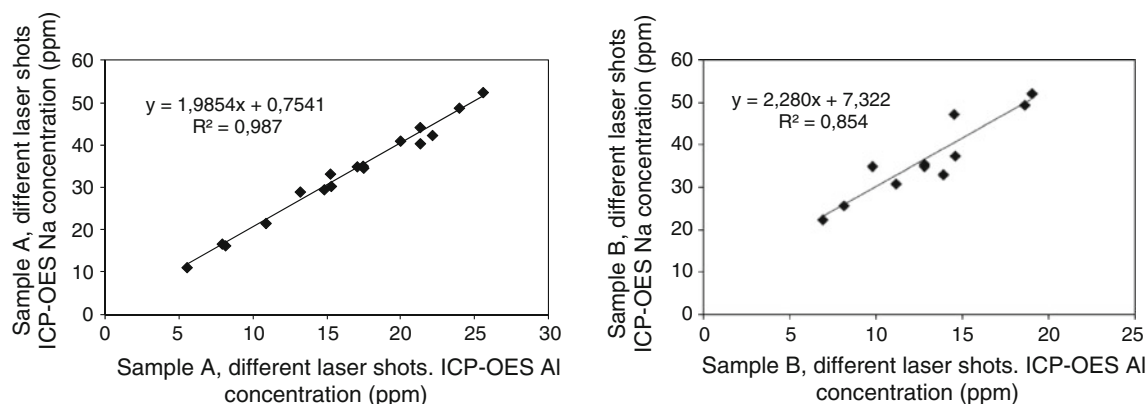


Fig. 8 Na/Al concentration ratios for LP-LA cryolite A and B samples

ratios were obtained by ICP-OES for different sub-samples after a varying number of laser shots were applied to the samples studied. The corresponding results are summarized in Fig. 8, where error bars are not included as their values were well below 5 % (standard deviation of 3 replicas).

Although this analytic technique allows the precise quantification of the concentration of the measured LP-LA solutions, the difficulty in determining the extracted mass from the samples in each case cause that the values obtained can be interpreted only as relative concentrations. Attempts were made to measure the elemental concentrations of the ablated material in the slurry by weighting the cryolite samples before and after ablation to derive the composition of the bulk. However, in spite of the large pit produced by LP laser ablation, the amounts of removed mass are in the range of a couple of milligrams, which are too small for accurate weighing. Fortunately once again the value of interest, the elemental ratio Na/Al, is not affected by this limitation.

The sample A was the most homogeneous one, and in this case the Na/Al ratio obtained was 1.99 ± 0.06 , which represents a result with a 3 % uncertainty. This range of precision is enough for industrial applications, including the optimization in the addition of alumina to the electrolytic Hall-Herault reduction cells.

On the other hand, the sample B was mechanically more fragile and inhomogeneous. In this case the measured Na/Al ratio was 2.28 ± 0.31 , which represents a result with 14 % of uncertainty. The relative insufficient precision of this measurement is related to the heterogeneity of the sample so that care to ensure homogeneity of the material to be analysed is advised.

4 Conclusions

The composition and relative elemental concentrations of cryolite samples from Hall-Herault aluminium production

cell were obtained by combining liquid phase laser ablation with three different analytical techniques. The procedure is an easy and fast way of obtaining nanoparticle suspensions which has significant advantages in comparison with the usual expensive and time-consuming digestion or fusion methods used for this purpose.

The optical analysis and images obtained by SEM confirm that the extracted material has a particulate fraction with sizes in the tenths of micron and submicron down to nanometer scale range. The use of the focalized electron beam from the SEM to produce X-ray fluorescence of the dried suspensions confirmed that particles of cryolite are extracted. While the dissolved and the nano-particulate fractions lead to a homogeneous suspension, the bigger particles make it relatively heterogeneous. This is the most probable cause of the dispersion in the relative concentrations shown in Table 1, even for samples produced with the same number of shots.

The results obtained by TXRF show that the concentration of minor and traces elements in the liquid varies correspondingly with the number of laser shots. With the conditions used and for 50 shots these concentrations are well below 10 ppm.

Regarding the Na/Al ratio determination, by ICP-OES, the results indicate that the technique has the potential for industrial cell diagnostics as it was indeed possible to discriminate between different samples, type A and B in this case, their corresponding ratios being 1.99(3 %) and 2.28(14 %). It is advised that care must be taken to ensure homogeneity of the samples taken from Hall-Herault reduction cell baths, since sample inhomogeneity appear to be the main cause of the relatively high uncertainty observed for the Na/Al ratio in Sample B. We believe the technique reported of LP-LA opens up a new procedure for analysis of difficult materials. However, further work has to be done to develop procedures for accurate quantification of the particle suspensions produced.

Acknowledgments We thank the Dean of Research and Development of the Simon Bolivar University (DID-USB) for the funds to acquire the Nd:YAG Laser used for this study. Also we thank Mr. Gleen Rodriguez for the sample preparation, SEM images and XRF microanalysis.

References

1. J.S. Becker, Applications of inductively coupled plasma mass spectrometry and laser ablation inductively coupled plasma mass spectrometry in materials science. *Spectrochim. Acta B.* **57**, 1805–1820 (2002)
2. J. Koch, A. von Bohlen, R. Hergenröder, K. Niemax, Particle size distributions and compositions of aerosols produced by near-IR femto- and nanosecond laser ablation of brass. *J. Anal. At. Spectrom.* **19**, 267–272 (2004)
3. J. Koch, H. Lindner, A. von Bohlen, R. Hergenröder, K. Niemax, Elemental fractionation of dielectric aerosols produced by near-infrared femtosecond laser ablation of silicate glasses. *J. Anal. At. Spectrom.* **20**, 901–906 (2005)
4. S.M. Eggins, Laser ablation ICP-MS analysis of Geological materials prepared as lithium borate glasses. *Geostand Geoanal Res Vol* **27**, 147–162 (2007)
5. X. Mao, R.E. Russo, Optimization and calibration of laser ablation–inductively coupled plasma atomic emission spectrometry by measuring vertical spatial intensity profiles. *J. Anal. At. Spectrom.* **12**, 177–182 (1997)
6. R.E. Russo, X.L. Mao, O.V. Borisov, Liu. Haichen, Influence of wavelength on fractionation in laser ablation ICP-MS. *J. Anal. At. Spectrom.* **15**, 1115–1120 (2000)
7. D. Bleiner, D. Günther, Theoretical description and experimental observation of aerosol transport processes in laser ablation inductively coupled plasma mass spectrometry. *J. Anal. At. Spectrom.* **16**, 449–456 (2001)
8. D. Bäuerle, *Laser processing and chemistry*, 3rd edn. (Springer, Berlin, 2002)
9. I. Ozerov, A.V. Bulgakov, D.K. Nelson, R. Castell, W. Marine, Production of gas phase zinc oxide nanoclusters by pulsed laser ablation. *Appl. Surf. Sci. Vol* **247**, 1–7 (2005)
10. Roland. Hergenröder, Ota. Samek, Vanja. Hommes, Femtosecond laser ablation elemental mass spectrometry. *Mass Spectrom. Rev.* **25**(4), 551–572 (2006)
11. C. Carmen, A. Garcia, H. Lindner, K. Niemax, Transport efficiency in femtosecond laser ablation inductively coupled plasma mass spectrometry applying ablation cells with short and long washout times. *Spectrochim. Acta B.* **62**, 13–19 (2007)
12. L. Yang, P.W. May, L. Yin, J.A. Smith, K.N. Rosse, Growth of diamond nanocrystals by pulsed laser ablation of graphite in liquid. *Diam. Relat. Mater.* **16**, 725–729 (2007)
13. K. Sasaki, Noriharu. Takada, Liquid-phase laser ablation. *Pure Appl. Chem.* **82**(6), 1317–1327 (2010)
14. K. Sasaki, Liquid-phase laser ablation. in *Proceedings ISPC 19*, Bochum, 2009, ed. by A. von Keudell, J. Winter, M. Böke, V. Schulz-von der Gathen. Accessed 7 May 2011. <http://www.ispc-conference.org/ispcproc/papers/661.pdf>
15. L. Yang, *Self Assembly and Ordering Nanomaterials by Liquid-Phase Pulsed Laser Ablation. Chapter 2: Liquid-Phase Pulsed Laser Ablation*. PhD Thesis, November 2007. School of Chemistry, University of Bristol. UK. Accessed 7 May 2011. <http://www.chm.bris.ac.uk/pt/diamond/lithesis/Chapter%202.pdf>
16. M. Manrique, Lecture course “Tecnología del Aluminio” MT-3317. Departamento de Ingeniería de Materiales, USB. (Caracas, Venezuela, 1999)
17. U. Grjotheim, H. Kvande, *Introduction to Aluminium Electrolysis. Understanding the Hall-Heroult Process* (Aluminium Verlag GmbH, Germany, 1993)
18. S. Prasad, Studies of the Hall-Heroult aluminium electrowinning process. *J. Braz. Chem. Soc.* **11**(3), 245–250 (2000)
19. E. D. Greaves, L. Sajo-Bohus, M. Manrique, C. DeArriba, Radioisotope neutron activation analysis of cryolite-alumina solution. *Acta Physica et Chimica Debrecina* 38–39:175–183 (2005)
20. J.B. Wang, C.Y. Zhang, X.L. Zhong, G.W. Yang, Cubic and hexagonal structures of diamond nanocrystals formed upon pulsed laser induced liquid-solid interfacial reaction. *Chem. Phys. Lett.* **361**, 86–90 (2002)
21. C.I. Prince, J. Kosler, D. Vance, D. Gunther, Comparison of laser ablation ICP-MS and isotope dilution REE analyses—implications for Sm–Nd garnet geochronology. *Chem. Geol.* **168**, 255–274 (2000)
22. R.C. Smith, K.S. Baker, Optical properties of the clearest natural waters (200–800 nm). *Appl. Opt.* **20**(2), 177–184 (1981)